Interactions between planar stiff polyelectrolyte brushes

Aaron Wynveen and Christos N. Likos

Institute for Theoretical Physics II: Soft Matter, Heinrich-Heine-Universität Düsseldorf, D-40225 Düsseldorf, Germany

(Received 25 March 2009; published 31 July 2009)

Molecular-dynamics simulations were performed for two opposing flat surfaces sparsely grafted with rigid polyelectrolyte chains whose lengths are smaller than their persistence lengths. The resulting force-distance dependence was analyzed theoretically in terms of two separate physical mechanisms: the pressure arising from osmotically active counterions trapped within the brush and the work required to bend the brush chains under confinement, which can be accurately characterized by a ground-state theory of rigid polymer buckling. These contributions are of the same magnitude and should be distinguishable in experiments of double-stranded DNA brushes.

Flexible rodlike polymers such as viral segments [1,2], actin [3], DNA [4,5], magnetic filaments [6], and carbon nanotubes [7] have emerged as novel physical systems that can be engaged in a variety of ways to influence material properties in different physical applications. Of particular importance to soft matter science is the possibility of grafting them on planar or curved, rigid or flexible surfaces, creating thereby new kinds of colloidal particles. Flexible filaments can be regarded as nanosprings [8] and the effects of their rigidity in inducing buckling transitions either of the chains themselves [9,10] or of the flexible surface on which they are grafted [3] have been quantitatively analyzed. An alternative possibility to induce rigidity on otherwise flexible grafted polymers is by electrical charge. The resulting polyelectrolyte (PE) brushes have recently garnered a great deal of attention [11–13]. Most of this attention has been paid to single brushes, e.g., in studies of the transition of a brush in the "osmotic" regime [14,15], in which the osmotic stress of trapped counterions within a brush swells the brush chains, to a collapsed state with added salt [16–18]. Considerable work has also been initiated to explore interactions between brushes [19–23]. The combined effect of *intrinsic* rigidity and charge, however, has received little attention to date. In the very recent work of Huang *et al.* [2], charged M13 viruses were grafted on colloidal particles and the ensuing forces were analyzed only at intersurface distances for which the chain compression contribution does not set in, employing a theory of the osmotic pressure of the counterions [23].

Recently, experiments studying the interactions between brushes sparsely grafted with rigid PEs, such as DNA, have been carried out [4]. Unlike their densely grafted counterparts, interdigitation of chains on opposite brushes may occur. This interpenetration leads to a force-distance dependence for sparsely grafted brushes that is quite different from the predictions for densely grafted brushes in the osmotic regime. By direct comparison with laser-tweezer force measurements, it has been argued [5] that the counterion-entropy contribution [23] is not sufficient to describe the interbrush forces and that a compression contribution from the chains being pressed on the surface of the opposite colloid is present. The latter has been modeled by the force arising from the uniaxial compression of a charged, stiff PE rod, giving rise to excellent agreement with experimental results [5]. Notwithstanding this fact, a more realistic description of

the conformational changes in a stiff PE chain should entail the possibility of *bending* of the same upon approach toward a planar hard surface. In this Rapid Communication we pursue precisely this goal. We present simulation results of brushes sparsely grafted with rigid, short PE chains and develop an accurate theory for their interactions. Being that the chains are shorter than their natural persistence lengths, we find that, besides a contribution to the force of osmotically active counterions trapped in the brushes, we must include an additional force term arising from the finite rigidity of the chains and we quantitatively describe both by means of accurate theoretical approaches.

Molecular-dynamics simulations (see Ref. [24] for details) were performed for flat brushes each consisting of 42 PE chains of N monomers of unit charge, corresponding monovalent counterions to neutralize the brushes, and no added salt. Chain monomers and counterions were modeled as beads with an effective steric radius $a=11$ Å, the approximate radius of DNA used in cell model calculations to accurately fit osmotic pressure experiments of columnar DNA assemblies [25,26], for chain-counterion interactions. Adjacent chain monomers were bonded by a harmonic potential with an equilibrium length of $b=3.4$ Å and stiffness was provided by a harmonic angle potential with a bending force constant used in previous studies [24,27] that gives the approximate persistence length of DNA at low ionic strength, ~ 500–1000 Å [28]. Note that electrostatic repulsion among monomers on the same chain also contributes to the persistence length, and therefore the latter depends very much on its ionic environment [28–30]. Furthermore, the same stiffness was accorded to the grafting points, effectively clamping the chains perpendicular to the grafting surface, which resulted in chains at the edge of the brush having similar or parallel conformations to those in the center.

Chains were periodically grafted at one end to each opposing, impenetrable wall in the simulation cell with grafting points on opposite walls staggered by half the lattice spacing. The grafting density σ corresponded to an average nearest-neighbor distance equal to an $N=50$ monomer chain length L. The total cross-sectional area ($L_x \times L_y$, with the brush normal to the z direction) of the simulation box was greater, by a factor of 4 or more, than the grafting area, which allowed for a fraction of the counterions to be free of the brushes. The total accessible volume V ($L_x \times L_y \times D$, with $L_x = L_y$

$=\sqrt{V/D}$) was kept constant as the distance D between the brush walls was varied, hence guaranteeing that the average counterion density remained the same across simulations. With this geometry, we are better able to imitate experiments of finite brushes in a dilute background solution as well as to probe how the counterion population within the brush varied with brush separation. L_z of the full simulation box was chosen to be much larger than ($>3\times$) D and a correction term for this slab geometry was included [31] to eliminate the effect of interactions between periodic replicants in the z direction. Two trials were carried out for chains composed of either $N=30$ ($L=102$ Å) or $N=50$ ($L=170$ Å) monomers with the same accessible system volume, $V=12\times10^5$ nm^3, for each.

The calculated pressure on each brush consisted of the force on the brush wall due to counterions, Π_{osm}, as well as the force at the grafting points of the chains and that of the buckled chains of the opposite brush on the grafting wall, Π_{chain}, giving a total pressure $\Pi=\Pi_{osm}+\Pi_{chain}$. Being that sparse brushes of stiff chains are completely interpenetrating [21], as opposed to studies of brushes with flexible PEs and/or with large grafting densities, this latter contribution is realized when chains make contact with the opposite wall, i.e., when $D<L$.

This component to the total force may be determined by calculating the bending energy of a buckled inextensible chain [32,33], $V_{bend}=(B/2)\int_0^L[d\mathbf{t}(s)/ds]^2ds$, where B is the bending rigidity modulus and $\mathbf{t}(s)$ is the tangent vector to the contour at contour length s. This must be minimized subject to the condition that the ungrafted end of the chain lies at the opposite wall without penetrating it, that is $\int_0^L\mathbf{t}(s)\cdot\mathbf{z}\,ds=D$ where $\mathbf{z}$ is the unit vector perpendicular to the brush wall. The chain conformation minimizing the bending energy is found by solving the corresponding Euler-Lagrange equations, which are given in Refs. [33,34]. However, in contrast to the very similar solutions with the boundary conditions of a chain clamped at both ends [33,34], we determine solutions for a chain that is free at its ungrafted end. The solution takes different forms about a critical distance [34] $D^*/L=2E[1/2]/K[1/2]-1=0.4569\dots$ (where $K[m]$ and $E[m]$ are the complete elliptic integrals of the first and second kinds, respectively): (i) when $D>D^*$, the chain's curvature is finite throughout its contour length becoming zero only at its free end; and (ii) when $D<D^*$, a segment of length $(1-D/D^*)L$ at the end of the chain lies flat against the opposing surface. For the latter, the shape of the chain up to this flat segment has the same form, with the contour location s rescaled by D/D^*, as the chain conformation when $D=D^*$.

Once the chain conformation is known, the bending energy and the force between the brushes due to bending of the chains may be found:

$$F_{bend}(D)=\begin{cases}\dfrac{\pi}{2}\dfrac{B}{L}\dfrac{D^*}{D^2} & \text{if } D<D^* \\ K^2[m]\dfrac{B}{L^2} & \text{if } D^*<D<L,\end{cases} \quad (1)$$

where m is a solution to $2E[m]/K[m]-1=D/L$. At $D=L$, when the chains first contact the opposite wall, the force
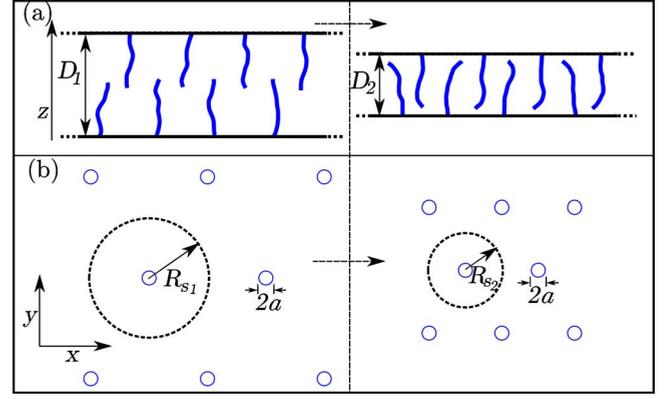

FIG. 1. (Color online) A schematic diagram of the (a) brushes and (b) their mapping onto a 2D cell model at two different brush separations. As the separation between the brushes is reduced, the corresponding cells are shrunk, $R_{s_2}/\sqrt{D_2}=R_{s_1}/\sqrt{D_1}$, in the 2D mapping to mimic the correct chain density of the brushes of the original 3D system.

jumps abruptly from zero to a finite value, $K^2[0]B/L^2=(\pi/2)^2B/L^2$. The chain contribution to the total pressure is thus given by $\Pi_{chain}=\sigma F_{bend}$.

For densely grafted brushes in the osmotic regime [13,14,35], nearly all counterions are confined within the brushes. If the density of the counterions at a brush wall corresponds to a fraction f of the average density of counterions within the entire brush, the osmotic pressure at separations $D<2L$ is given by [22]

$$\Pi_{osm}^{ideal}=fk_BTN\sigma[D(1-\eta)]^{-1}, \quad (2)$$

where the term in the brackets is a correction for the excluded volume fraction $\eta=\pi a^2L\sigma/D$ of the chains within the brush. Assuming that the counterion density within the brush was uniform, f would be unity. This assumption, however, is not valid for the sparse brushes we consider. For a finite charged line, the electrostatic potential near the center of the line is nearly twice that near its end, and thus, the counterion population is much less at the grafting wall than in the center of the brush. This argument can be recast in terms of counterion condensation on the strong (having a Manning parameter $\xi>1$ [36]) PE chains. Although any finite PE would lose all its counterions under infinite dilution, studies [37–41] demonstrate counterion condensation on finite chains in the semidilute regime of our brushes. Furthermore, it was shown that fewer counterions condense at the ends of the chain than at the center [38], so for simplicity, based on this study, we approximate that the counterion density at the brush wall is half its average value, $f=1/2$.

We have also determined the osmotic pressure contribution by mapping the sparse brush problem onto a two-dimensional (2D) cell model for infinite charged rods [42,43] (see Fig. 1). Here we assume that the pressure at the cylindrical cell boundary of the PE chain is equivalent to the pressure at the brush walls. Indeed, Antypov and Holm [41] demonstrated that for the finite cylindrical cell which provides the lowest free energy in a system of rodlike PEs and fully neutralizing counterions, the *average* counterion den-

sity, and hence the osmotic pressure, at the lateral cell wall is the same as that at the ends of the cell. Although our system is quite different from theirs [41], and we employ a cylindrical cell with a geometry fixed by the distance between the brush walls and by the grafting density, we find that such a treatment yields another means by which to obtain the osmotic pressure contribution while also providing a quantitative comparison of the counterion distributions about the brush chains.

For our problem, we assume the chains in each cell are fully neutralized by the counterions in our closed (periodic) system, and so the electrostatic interaction between brushes is quite weak before the chains begin to interdigitate at $D=2L$. Hence we solve the nonlinear Poisson-Boltzmann equation

$$\epsilon \nabla^2 \varphi(\mathbf{r}) = -4\pi e n_{C^+} \exp[-\beta e \varphi(\mathbf{r})], \qquad (3)$$

where $\beta = (k_B T)^{-1}$, with the boundary conditions

$$a(\partial \varphi / \partial r)|_{r=a} = 2e/(\epsilon b) \text{ and } R_s(\partial \varphi / \partial r)|_{r=R_s} = 0, \qquad (4)$$

which has been solved analytically in previous works (see, e.g., Refs. [25,35,42,43]) and which may be modified if full neutralization of the line charges is not assumed [40]. Here r is the radial coordinate, e is the unit charge, n_{C^+} is the average counterion concentration, a is the effective radius of the chain, and, again, b is the distance between unit charges along the chain. The original brush system is then translated into this 2D formulation by scaling the radius of the cell boundary in the cell model with the distance between the walls of the original three-dimensional (3D) brush system, $R_s = \sqrt{D/(2\pi L\sigma)}$ (Fig. 1).

Comparisons of the counterion concentration about a chain between this implementation of the cell model and simulations for different brush separations are shown in Fig. 2. Although the cell model is a mean-field theory and the change in brush separation is modeled solely by changing the location of the cell boundary, the larger amplitude at the chain surface and the initial decay near the chains of the counterion density with decreasing D is well described by the cell model without taking into account the counterion correlation effects underlying counterion condensation at the surface of the strong PE chains. Via the argument that the average counterion distribution at the cell boundary is the same at the end of the cell (the brush wall here) [41], the cell model predicts an osmotic pressure between the brushes of $\Pi_{osm}^{cell} = n_{C^+} k_B T \exp[-\beta e \varphi(R_s)]$.

Results of the simulation and theory are presented in Fig. 3 for the two different chain lengths. As predicted by the theory for bending of stiff chains, the pressure jumps at the location $D=L$. We find that a slightly larger bending rigidity modulus B is required to fit the chain contribution to the pressure of the brushes with smaller ($N=30$ monomer) chains, resulting from an effective larger persistence length for these shorter brushes associated with the discreteness of the chains. The force resulting from chain bending constitutes a larger share of the total force for shorter chains as well.
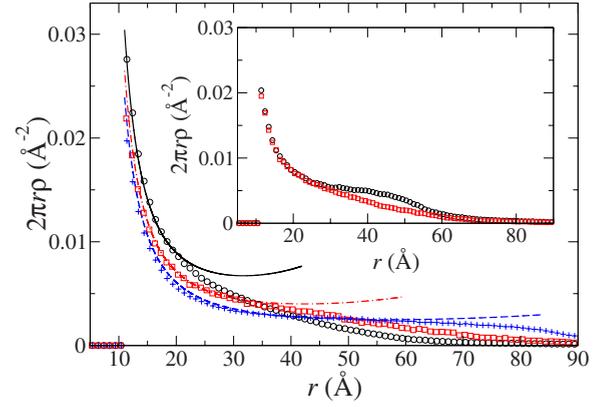

FIG. 2. (Color online) The distribution of the counterions' shortest distance to a (bent) brush chain averaged over the entire length of a chain. Simulation results are shown for the $N=50$ monomer chain at brush separations of $D/L=0.44$ (circles), $D/L=0.88$ (squares), and $D/L=1.76$ (crosses). The corresponding cell model calculations of the radially dependent counterion densities (lines) for these separations, where $R_s = \sqrt{D/(2\pi L\sigma)}$, are also illustrated. Inset: the radial distribution of the counterions about only the grafted ends of the chains for $N=30$ (circles) and $N=50$ (squares) for $D/L=0.44$, demonstrating the larger population of the counterions at the brush wall for the shorter chains.

For the osmotic counterion contribution, we assumed that the number of counterions within the brush remained constant as D was varied. This assumption, confirmed by the simulations, is based on theory demonstrating that the osmotic coefficient, and hence the net charge, of a brush was invariant to a change in the cell size enclosing the brush [23]. Again, the counterion density at the brush wall, providing the osmotic pressure, is less than the average density within the
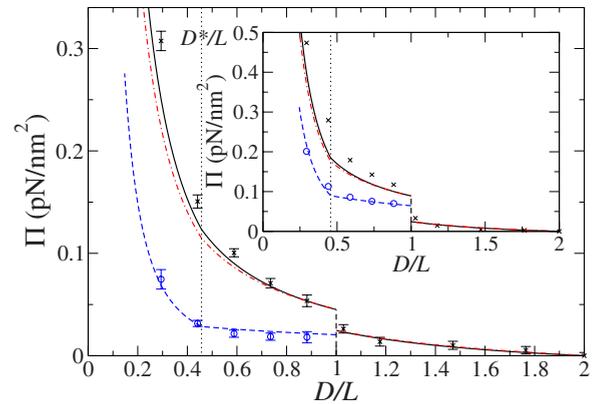

FIG. 3. (Color online) Simulation and theory results for the pressure between brushes as a function of their separation for the $N=50$ ($N=30$, inset) monomer chains. The total pressure ($\times$ symbols), relative to their values at $D=2L$, and the contribution only due to the chains (circles) for the simulations are shown. The bending contribution, Eq. (1), is given by the dashed (blue) line with $B=3.0\times10^{-28}$ J m ($B=3.4\times10^{-28}$ J m, inset). The sum of this contribution and that due to the counterions is shown by the dashdot (red) ($\Pi_{chain}+\Pi_{osm}^{ideal}$) and solid (black) ($\Pi_{chain}+\Pi_{osm}^{cell}$) lines. The dotted vertical line indicates where the bending behavior changes (D^*/L).

brush, and so f in Eq. (2) was approximated as being 1/2. In the cell model, the chain's charge in the interior of the brush is judged to be neutralized by the counterions, which has also been ascertained from simulations, and so no fitting parameters are required. For the shorter chains at close confinement, the infinite chain (2D) approximation of the cell model underestimates the counterion contribution to the overall pressure since finite-size effects for the smaller chains become more important. Here, proportionately larger sections of the ungrafted ends of a brush are compressed against the opposite brush wall, increasing the average counterion density, and hence osmotic pressure, at the wall (see inset of Fig. 2).

In summary, simulations and a theoretical treatment have been completed for sparse brushes of short PE chains with finite rigidity. Unlike densely grafted brushes of flexible PEs, the force between the brushes investigated here not only arises from the osmotic stress of compressed counterions within the brush but also results from the work required to bend the rigid chains. The contribution to the total force arising from chain bending is of the same order as this osmotic term and may even dominate it at increased confinement as the bending contribution scales as $1/D^2$. Interestingly enough, this is the same law as the simple compression mechanism put forward in Ref. [5], demonstrating the insensitivity on the precise form of chain deformation. Our analysis offers a unique quantitative description of the interactions between PE brushes with rigid chains that may be exploited, e.g., for statistical mechanical studies of multibrush systems and/or for their many physical applications, such as colloidal stabilization and lubrication, as well as control of electrical conductivity of nanoparticle films [44].

[1] C. Mao *et al.*, Science **303**, 213 (2004).

[2] F. Huang *et al.*, Phys. Rev. Lett. **102**, 108302 (2009).

[3] E. Helfer *et al.*, Phys. Rev. Lett. **87**, 088103 (2001).

[4] K. Kegler, M. Salomo, and F. Kremer, Phys. Rev. Lett. **98**, 058304 (2007).

[5] K. Kegler *et al.*, Phys. Rev. Lett. **100**, 118302 (2008).

[6] C. Goubault *et al.*, Phys. Rev. Lett. **91**, 260802 (2003).

[7] A. Cao *et al.*, Nature Mater. **4**, 540 (2005).

[8] A. F. da Fonseca and D. S. Galvão, Phys. Rev. Lett. **92**, 175502 (2004).

[9] L. Golubović, D. Moldovan, and A. Peredera, Phys. Rev. Lett. **81**, 3387 (1998).

[10] P. Ranjith and P. B. Sunil Kumar, Phys. Rev. Lett. **89**, 018302 (2002).

[11] E. P. K. Currie *et al.*, Adv. Colloid Interface Sci. **100-102**, 205 (2003).

[12] J. Rühe *et al.*, Adv. Polym. Sci. **165**, 79 (2004).

[13] A. Naji *et al.*, Adv. Polym. Sci. **198**, 149 (2006).

[14] P. Pincus, Macromolecules **24**, 2912 (1991).

[15] O. V. Borisov *et al.*, J. Phys. II **1**, 521 (1991).

[16] N. A. Kumar and C. Seidel, Macromolecules **38**, 9341 (2005).

[17] Y. Mei *et al.*, Phys. Rev. Lett. **97**, 158301 (2006).

[18] Y. Mei, M. Hoffmann, M. Ballauff, and A. Jusufi, Phys. Rev. E **77**, 031805 (2008).

[19] M. Balastre *et al.*, Macromolecules **35**, 9480 (2002).

[20] U. Raviv *et al.*, Nature (London) **425**, 163 (2003).

[21] O. J. Hehmeyer and M. J. Stevens, J. Chem. Phys. **122**, 134909 (2005).

[22] N. A. Kumar and C. Seidel, Phys. Rev. E **76**, 020801(R) (2007).

[23] A. Jusufi *et al.*, Colloid Polym. Sci. **282**, 910 (2004).

[24] C. N. Likos *et al.*, J. Phys.: Condens. Matter **20**, 494221 (2008).

[25] P. L. Hansen, R. Podgornik, and V. A. Parsegian, Phys. Rev. E **64**, 021907 (2001).

[26] A. A. Kornyshev *et al.*, Rev. Mod. Phys. **79**, 943 (2007).

[27] P. S. Crozier and M. J. Stevens, J. Chem. Phys. **118**, 3855 (2003).

[28] J. F. Marko and E. D. Siggia, Macromolecules **28**, 8759 (1995).

[29] T. Odijk, J. Polym. Sci., Polym. Phys. Ed. **15**, 477 (1977).

[30] J. Skolnick and M. Fixman, Macromolecules **10**, 944 (1977).

[31] I.-C. Yeh and M. L. Berkowitz, J. Chem. Phys. **111**, 3155 (1999).

[32] T. Odijk, J. Chem. Phys. **108**, 6923 (1998).

[33] M. Emanuel, H. Mohrbach, M. Sayar, H. Schiessel, and I. M. Kulic, Phys. Rev. E **76**, 061907 (2007).

[34] A. E. H. Love, *A Treatise on the Mathematical Theory of Elasticity*, 2nd ed. (Cambridge University Press Warehouse, London, 1906).

[35] A. Naji *et al.*, Eur. Phys. J. E **12**, 223 (2003).

[36] G. S. Manning, J. Chem. Phys. **51**, 924 (1969).

[37] G. V. Ramanathan and J. C. P. Woodbury, J. Chem. Phys. **77**, 4133 (1982).

[38] T. Odijk, Physica A **176**, 201 (1991).

[39] P. González-Mozuelos and M. Olvera de la Cruz, J. Chem. Phys. **103**, 3145 (1995).

[40] A. Deshkovski, S. Obukhov, and M. Rubinstein, Phys. Rev. Lett. **86**, 2341 (2001).

[41] D. Antypov and C. Holm, Phys. Rev. Lett. **96**, 088302 (2006).

[42] T. Alfrey *et al.*, J. Polym. Sci. **7**, 543 (1951).

[43] R. M. Fuoss *et al.*, Proc. Natl. Acad. Sci. U.S.A. **37**, 579 (1951).

[44] J. Im *et al.*, Langmuir **25**, 4288 (2009).